RZ 3595 (# 99605) 07/18/2005
Electrical Engineering 17 pages

Research Report

Physical Layer Modelling for Reader Scenario

Martin Weisenhorn

IBM Research GmbH
Zurich Research Laboratory
8803 Rüschlikon
Switzerland

Physical Layer Modelling for Reader Scenario

Martin Weisenhorn
IBM Zurich Research Laboratory

June 8, 2005

Contents

Abstract

One objective of the Task group WP3b5 of the PULSERS project in framework FP6 is to suggest a medium access (MAC) Layer for a sensor network. The performance of this MAC layer depends on physical layer (PHY) properties. A reliable performance characterization of the MAC requires a joint evaluation of PHY and MAC. In this work, both, a suitable PHY and a MAC layer are proposed. Essentially, the PHY layer comprises packet oriented transmission of 2PPM UWB signals and noncoherent reception. The MAC layer performs random channel access of uncoordinated transmitters, implying the presence of multiuser interference. A semi-deterministic model of the PHY layer is developed, which considers multiuser interference in an accurate fashion and is suited as a part of an efficient PHY-MAC cross layer simulator.

1 Introduction

The goal of this work is to develop an efficient simulator for the physical layer of a communication link. The modulation scheme used is 2PPM, the receiver is noncoherent and interference

from uncoordinated users is taken into account. The purpose of this simulator is to be part of a cross layer simulator for the medium access (MAC) layer and physical (PHY) layer. The considered communication scenario (called Reader scenario in the context of this project) comprises a cluster of sensors that transmit data packets via a wireless UWB communication link to one ore more receivers, called cluster heads. Expected features are the following: The data rate per communication link is 1 Kbit/s or lower. The sensors should be battery driven and have a lifetime of several years. To meet these expectations, the sensors must operate at very low power, with current or near future technology this can be achieved only if the sensors have no receiver, i.e., the communication links from the sensors to the cluster heads are unidirectional. Another requirement is that the cluster heads consume as view power as possible and contain a receiver with minimal complexity.

Because of the unidirectional communication links, the sensors have to share a common channel in an uncoordinated fashion. There are several known multiple access methods that are suited for such operation, DS-CDMA, TH-PPM, RDMA, and random access. By random access we understand that each user transmits data packets at randomly chosen time instants, more specifically, the transmission times of the packets are chosen according to a poisson process. The poisson processes of the individual users are statistically independent. Note, that this random access scheme can work with a single receiver. In the case when more than one packet arrives at the receiver at the same time, both packets are lost in the worst case. The rate of packet collisions can be kept low by choosing a small enough data traffic. An important drawback of the random access scheme shares without feedback channel, is that a successful reception of data packets cannot be guaranteed as retransmission requests are not possible. However the probability of successive packet communication can be increased by the use of coding or in the simplest case, by m-fold retransmission of each data packet by the sensors. In this work, we focus on random access to keep the receiver complexity low, note that the relatively small throughput offered by the random access method is satisfying. The other multiple access schemes mentioned are more complex, as they require at least N receivers that work in parallel for the simultaneous reception of N sensor signals, as a result of this added complexity, these receivers can receive data packets from differen users, simultaneously.

A cluster head would achieve the best performance by the use of a coherent receiver with channel estimation and a matched filter. The signal bandwidth of UWB signals however is high and thus also the complexity and power consumption of a channel estimator and matched filter. Furthermore, does a matched filter receiver require high synchronization precision, in the order of 0.1 ns [1], which again requires a fast tracking loop with high power consumption. Furthermore would the channel of each sensor to cluster head link have to be estimated. Channel estimation and precise synchronization does moreover require long preambles, such that the payload of the data packets would be reduced, this is in particular true for data packets containing few payload data. Because of these reasons we decided to employ a noncoherent receiver type, among which we can choose the transmitted reference receiver [2, 3] or the energy detector [4, 5]. Implementation of the transmitted reference receiver is difficult because of the required delay for the reference pulse, which is in the order of some tens of a nanosecond. No elegant method is yet known to the authors which can be used to realize such delays. In contrast, the energy detector can be implemented with relative ease in current standard CMOS technology. A further advantage of this receiver type is its low power consumption and the small required synchronization

precision, which is in the order of some nanoseconds. The energy detector, synonymously called the noncoherent receiver, cooperates well with PPM. For this work we choose a robust modulation scheme in favor of a higher data rate scheme, hence, we decide for 2PPM. As shown in [5], the average power and peak power emission values of plain 2PPM can be reduced by randomly flipping the polarity of the transmitted pulses of a PPM signal; this technique does not impact the performance of PPM in combination with noncoherent reception. Based on these considerations, the physical layer is roughly specified by the random multiple access scheme, the modulation scheme 2PPM with random pulse polarity, and a noncoherent receiver.

The research project wp3b5 plans the development of a cross layer simulator for the physical and the MAC layer. To get a significant statistics for characterizing the overall performance of the sensor network under discussion, the number of simulated packet transmissions per sensor should be in the order of one thousand. To run simulations in due time, the statistics of the signal and interference processed by the receiver, i.e., the decision variable statistics must be computed efficiently, and under consideration of the a realistic channel model. An interference model that ignores the details of the interference signal by only considering collisions of various strengh is given in [6]. The approach given in this work goes beyond this and yields more realistic results. E.g., assuming an interfering signal whose pulses are by accident placed at time instants such that the reception of the desired signal is not affected, the desired signal can still be received. However, in a collision based interference model this situation would result in transmission errors.

It has turned out that a C written simulation programm can achieve sufficient performance, such that the decision variables at the receiver can be computed directly on basis of the discrete time channel impulse responses. This method can however be improved, by computing a lookup-table with required intermediate results that can be reused several times during the reception of a data packet.

The physical layer consisting of transmitters and a receiver is specified in Section 2. The basic computations required to determine the decision variables is presented in Section 3. The desired user signal, the multiuser interference term and the noise term are computed separately. The noise term is shown to be gaussian distributed, which allows to specify a bit error probability (BEP) for each set of desired signal term and interference term. Specifying a BEP helps to reduce the number of required simulation runs. In a more complex alternative one would in addition generate a large number of noise realizations and determine the number of successfully transmitted bits within a packet. From these numbers, the BEP would be estimated.

Section 4 presents a method to simulate whether the synchronization was successive or not.

2 Physical Layer

2.1 Transmitter

As mentioned above, we propose to use binary pulse position modulation. The coded and scrambled binary symbols of the i-th sensor, $a_{i,k} \in \{0, 1\}$ modulate the transmitter signal, where the k-th symbol within a data packet directly determines the position of one UWB pulse. The shape of an individual pulse is defined by $g(t)$, which is the impulse response of an ideal bandpass filter with center frequency f_0 and Bandwdith B. $g(t)$ has energy 1, i.e., $\|g\|^2 = \int_{-\infty}^{\infty} g^2(t)\, dt = 1$.

The choice of an ideal bandpass filter $g(t)$ is justified, as it results in simpler analytical expressions for the signals in the receiver [5]; moreover, the results will not change much if another, more realistic bandpass filter is assumed. The transmitted signal is of the form

$$u_i(t) = \sqrt{E^{p,t}} \sum_{k=0}^{K-1} c_k \, g(t - kT - a_{i,k}\Delta_T - \tau_i) \tag{1}$$

and represents a data block which consists of K data symbols. Sensor i begins the transmission of the data block at time τ_i. The time interval available for the transmission of an individual symbol is T; the corresponding data symbol $a_{i,k}$ determines whether the pulse is transmitted at the beginning of this interval or with an offset Δ_T. To prevent intersymbol interference and to maintain the orthogonality of the received symbols, it is required that the delay Δ_T as well as $T - \Delta_T$ exceed the maximum channel delay spread τ_c or, equivalently, the support of the channel impulse response $b_{j,i}(t)$. Note that this condition limits the maximum data rate to $1/(2\tau_c)$. Index $j \in \{1, \cdots, N\}$ denotes the receiver and index $i \in \{1, \cdots, M\}$ denotes the transmitter. $b_{j,i}(t)$ generally represents the combined response of transmitter antenna, propagation channel, and receiver antenna [7]. Note that the symbol index k is different for different sensors; an explicit notion would give the symbol index k the subindex i of the sensor it belongs to, i.e., k_i; we skip this additional index for simplicity and because the notation presented in this work already prevents misinterpretations.

The energy per transmitted pulse is determined by the product $E^{p,t} = 2D_0BT$, where D_0 is the target two-sided power spectral density of the transmitted signal. The sequence $\langle c_k \rangle$, $c_k \in \{-1, +1\}$, is an i.i.d. pseudo-random binary sequence that randomizes the polarity of the transmitted pulses to smoothen the power spectrum of the signal $u_i(t)$; thus the power spectral density of the transmitted signal is proportional to the energy density spectrum of the transmitted pulse $g(t)$ [8]. As a noncoherent receiver is used (see Subsection 2.2) the sequence $\langle c_k \rangle$ does not need to be considered at the receiver and has no impact on it's performance. Without the sequence $\langle c_k \rangle$, the transmitter's power spectrum contains spectral lines, when applying the FCC's emission rules, this results in a reduction of the allowed energy per pulse if the pulse repetition frequency $1/T$ is larger than 1 MHz.

The choice of numerical values for the modulation parameters is left to a later stage of the project.

2.2 Noncoherent Receiver

The signal model of the noncoherent UWB radio receiver is depicted in Fig. 1. The induced signal at the feedpoint of the n-th receiver caused by the i-th sensor is given by the convolution $r_{n,i}(t) = b_{n,i}(t) * u_i(t)$. We assume that $b_{n,i}(t)$ is already limited to the signal bandwidth of $g(t)$, with the definition of $g(t)$ as an ideal bandpass filter response with unit energy, it follows that $b_{n,i}(t) * g(t) = b_{n,i}(t)/\sqrt{2B}$. The signal $r_{n,i}$ is schematically represented in Fig. 2. We assume that the propagation delay is contained in the beginning of transmission delay τ_i in (1), hence, the symbol $a_{i,k} = 0$ causes the received signal $r_{n,i(t)}$ to rise at time $t^1_{i,k} = kT + \tau_i$; the signal falls back to zero at time $t^2_{i,k} = t^1_{i,k} + \tau^c_{n,i}$, where $\tau^c_{n,i}$ is the total channel delay spread of $b_{n,i}(\eta, t)$. The symbol $a_{i,k} = 1$ causes the received pulse to arrive with the delay Δ_T, i.e., at

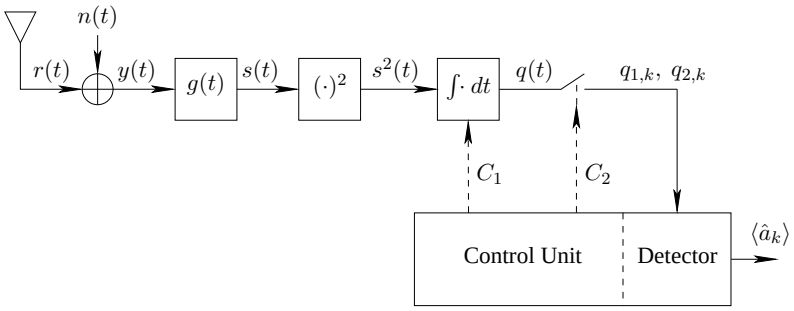

Figure 1: Noncoherent receiver structure.

$t^3_{i,k} = t^1_{i,k} + \Delta_T$, correspondingly the pulse falls back to zero at the time $t^4_{i,k} + \Delta_T$. The energy of the received pulse $r_{n,i}(t)$ is $E^r = \int [\sqrt{E_t}\, b_{n,i}(t) * g(t)]^2 dt$. We define the path gain of the channel as $\alpha_{n,i} = E_r/E_t = \int [b_{n,i}(t) * g(t)]^2 dt = \frac{1}{2B} \int [b_{n,i}(t)]^2 dt$, and hence, the path loss is $\alpha^{-1}_{n,i}($. To indicate that the path loss is an effect of the channel we define the normalized channel impulse response $\bar{b}_{n,i}(t) := b_{n,i}(t)/\alpha_{n,i}$, with energy $\int \bar{b}^2_{n,i}(t)\, dt = 2B$.

At the receiver n, the signals $r_{n,i}(t)$ of all sensors i are added up, i.e.,

$$r_n(t) = \sum_{i=1}^{M} r_{n,i}(t).$$

Finally the receiver noise, which is represented as a white Gaussian noise process $n_n(t)$ with two-sided power spectral density $N_0/2$, is added; the sum signal is

$$y_n(t) = n_n(t) + \sum_{i=1}^{M} r_{n,i}(t).$$

This signal is filtered by a band-limiting filter with impulse response $g_r(t) = \sqrt{2B} g(-t)$, who has gain 1 within the passband. The resulting signal $s(t)$ is the convolution of $g_r(t)$ with $y_j(t)$, i.e., $s(t) = g(t)_r * y_j(t)$. For simplicity, the receiver index j is skipped in the signal $s(t)$ and in the remaining part of the receiver description.

The square of the signal $s(t)$ is fed to an integrate and dump unit (IDU), formed by an integrator that is dumped by signal C_1 at time instant $t_s - T_I$. The output of this unit is sampled by signal C_2 at time instant t_s, i.e.,

$$q(t_s) = \int_{t_s - T_I}^{t_s} s^2(\tau) d\tau. \tag{2}$$

To obtain more insight into the properties of the IDU's output signal we split $s(t)$ into the sum $s(t) = \sum_{i=1}^{M} s_{r,i}(t) + s_n(t)$, where the term $s_{r,i}(t) = g(t) * r_{j,i}(t)$ is due to the sensor signals and $s_n(t) = g(t) * n_j(t)$ is due to the noise signal; for simplicity, the receiver index j is skipped in the signal $s(t)$ and the remaining part of the receiver description. With this we can write the

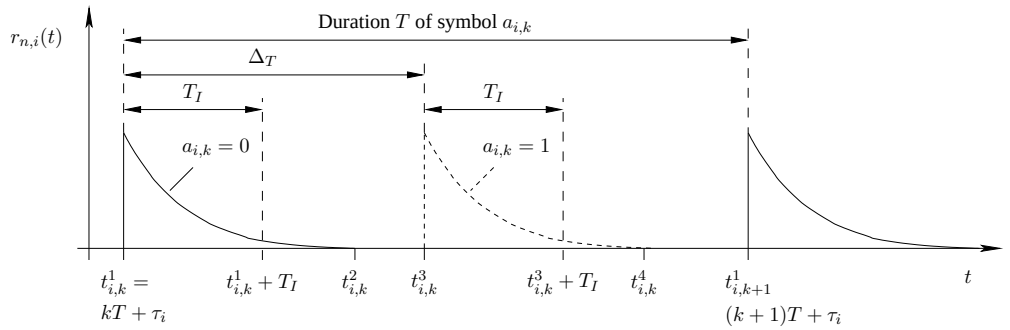

Figure 2: 2PPM visualized through average envelope of received signal $r_i(t)$ for the transmitted symbols $a_{i,k} = 0$, the dashed envelope is valid if $a_{i,k} = 1$. The channel delay spread is $t^2_{i,k}$-$t^1_{i,k}$=$t^4_{i,k}$-$t^3_{i,k}$.

IDU's sampled output (2) as

$$
\begin{aligned}
q(t_s) &= \int_{t_s-T_I}^{t_s} \left(\sum_{i=1}^{M} s_{r,i}(t) + s_n(t) \right)^2 dt \\
&= \int_{t_s-T_I}^{t_s} s^2_{r,1}(t) + \sum_{i=2}^{M} s^2_{r,i}(t) + \sum_{i=1}^{M} \sum_{\substack{l=1 \\ l\neq i}}^{M} s_{i,r}(t) s_{l,r}(t) + 2 s_n(t) \sum_{i=1}^{M} s_{r,i}(t) + s^2_n(t) dt \quad (3) \\
&= \nu(t_s) + \chi(t_s) + \psi(t_s) + \omega(t_s) + \zeta(t_s), \quad (4)
\end{aligned}
$$

$\nu(t_s) = \int_{t_s-T_I}^{t_s} s^2_{r,1}(t)\, dt$ denotes the signal component caused by sensor $i = 1$, without loss of generality we take sensor 1 as the desired sensor whose data is to be received. $\chi(t_s) = \int_{t_s-T_I}^{t_s} \sum_{i=2}^{M} s^2_{r,i}(t)\, dt$ is the squared interference term, $\psi(t_s) = \int_{t_s-T_I}^{t_s} \sum_{i=1}^{M} \sum_{l=1,l\neq i}^{M} s_{i,r}(t)\, s_{l,r}(t)\, dt$ is the mixed interference term, $\omega(t_s) = 2 \int_{t_s-T_I}^{t_s} s_n(t) \sum_{i=1}^{M} s_{r,i}(t)\, dt$ is the mixed signal-noise component, and $\zeta(t_s) = \int_{t_s-T_I}^{t_s} s^2_n(t)\, dt$ is the noise component. Figure 2 shows examples of the received signal $s_r(t)$ and the corresponding signal component $\nu(t)$ for an integration duration $T_I = 40$ ns with the noise $n(t) = 0$ and the interfering sensors $i = 2$ to M switched off.

To detect the k-th 2PPM symbol of sensor i, we use the heuristic approach of sampling the signal $q(t)$ twice per symbol, namely, at the two sampling instances $t_s = t^1_{i,k} + T_I$ and $t_s = t^1_{i,k} + \Delta_T + T_I = t^3_{i,k} + T_I$, where the position shift Δ_T is given by the modulation design (cf. Subsection 2.1). To maintain orthogonality we assume that $T_I < \Delta_T$. In practice, the sampling instants t_s would be provided by a synchronization unit at the receiver and would be chosen such, that depending on the transmitted data symbol $a_{i,k}$, the signal component $\nu(t)$ assumed its maximum value at one of the two sampling instances, see Fig. 3. Note that in general the samples $q^1_{i,k} := q(t^1_{i,k}+T_I)$ and $q^2_{i,k} := q(t^3_{i,k}+T_I)$ do not provide a sufficient statistics for the detection of the transmitted data sequence $\langle a_{i,k} \rangle$. However, we consider this approach justified because it allows a simple receiver implementation based on a single IDU. In fact it can be shown that the construction of a sufficient statistics could increase the receiver sensitivity by at most 6

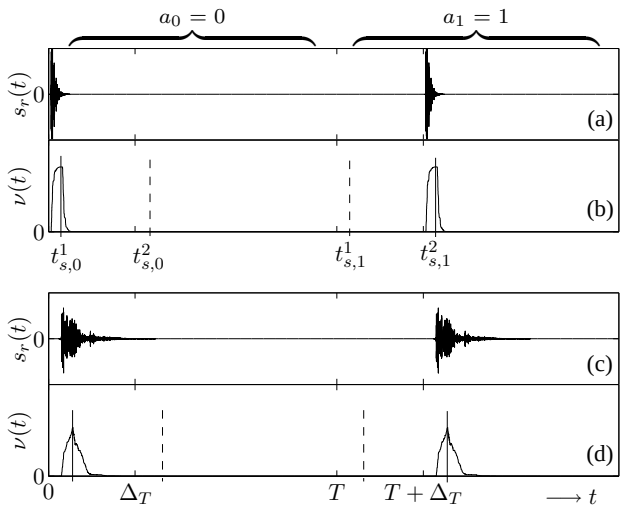

Figure 3: Received signal $s_r(t)$ and corresponding signal component $\nu(t)$ for the transmitted symbols $a_0 = 0$ and $a_1 = 1$; integration duration $T_I = 40$ ns, symbol period $T = 1$ μs, and position shift $\Delta_T = 0.3$ μs. Plots (a) and (b) show the signals for realization $m = 1$ of the channel model CM1, while plots (c) and (d) represent the signals for realization $m = 1$ of CM4; the channel models CM1 and CM4 are described in [7].

dB, while requiring a much higher receiver complexity.

We assume a maximum likelihood (ML) detector for single user detection, which bases its decision for the data symbol $\hat{a}_{i,k}$ on the samples $q^1_{i,k}$ and $q^2_{i,k}$. From the symmetry of the 2PPM scheme and because, by design, no intersymbol interference (ISI) is assuemd, it follows that the ML decision rule is given by

$$\hat{a}_{i,k} = \begin{cases} 0, \text{ for } q^1_{i,k} \geq q^2_{i,k}, \\ 1, \text{ otherwise.} \end{cases} \tag{5}$$

We introduce the decision variable $d_{i,k} := q^2_{i,k} - q^1_{i,k}$ for later considerations.

The random multiple access scheme is in a reasonable operating point, if most of the times when sensor i transmits a data block then the other sensors are quite, and we have $\chi(t_s) = \psi(t_s) = 0$ and the mixed signal-noise term simplifies to $\omega(t_s) = 2\int_{t_s - T_I}^{t_s} s_n(t) s_{r,1}(t)\, dt$ for $t_s = t^1_{i,k} + T_I$ as well as for $t_s = t^3_{i,k} + T_I$. In this case, i.e., where no multiuser interference deteriorates the signal quality, a reliable signal detection is granted for a sufficient received signal strength.

3 Semi Deterministic Physical Layer Model.

We assume sensor clocks that are not synchronized, but which have ideally precise clock frequencies. This implies that there is a limited number of patterns how interfering pulses can overlap,[1]

[1]The limited number of patterns is equivalent to the number of entries in the lookup-table, cf. the introduction.

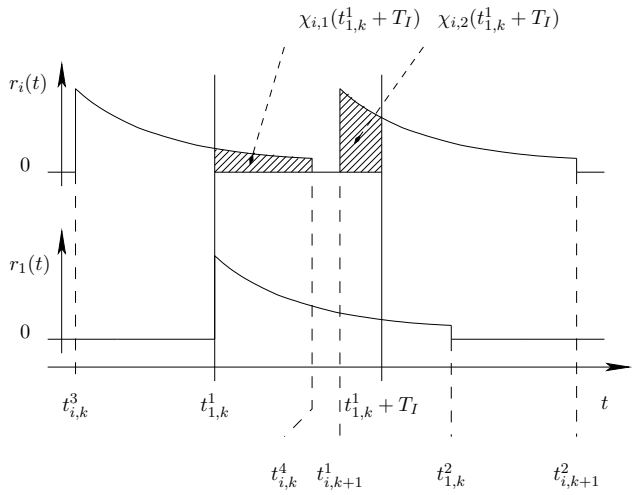

Figure 4: Schematic representation of desired signal $r_1(t)$ and interfering signal from sensor i, $r_i(t)$. In this example there are two shaded areas of the signal $r_i(t)$ contribute to the squared interference component, i.e., $\chi_i(t^1_{1,k}+T_I) = \chi_{i,1}(t^1_{1,k}+T_I) + \chi_{i,2}(t^1_{1,k}+T_I)$. The interfering pulse beginning at time $t^3_{i,k}$ carries the symbol $a_{i,k}=1$, while the pulse beginning at time $t^1_{i,k+1}$ carries the symbol $a_{i,k+1}=0$.

compare Fig. 4, 6, and 5. Computing the interference contribution at the integrator output requires the evaluation of an integral. For each possible interference pattern this has to be done only once, the result can be stored in a lookup table and be accessed if required. The mixed signal noise terms $\omega_{i,1}(ts)$ and $\omega_{i,2}(ts)$, and the noise only term $\zeta(ts)$ depend on the noise realization and can still be modelled as random variables with a specific distribution.

In this Section we discuss the individual components of the integral (4). Some of them are deterministic, some can be modelled as random variables, for this reason the resulting phy model carries the attribute *deterministic*.

As a first step we introduce the channel model used for our simulations.

3.1 Channel Model

We assume the channel model presented in [7]. An algorithm that creates channel realizations according to that model are included in [7] and available online. The channel model has parameters for the scenarios called CM1 to CM4, where CM1 is a LOS scenario for transmitter receiver distances between 3 and 5 m. CM4 is a non LOS (NLOS) scenario for transmitter to receiver distances between 5 and 10 m. A channel impulse response realization for both, CM1 and CM4 is depicted in Fig. 7. We denote a CIR realization by $b(t)$, which can be factorized into $b(t) = \alpha\bar{b}(t)$, where $\bar{b}(t)$ has energy $2B$ and α is the path gain, i.e. the ratio of the received to the transmitted pulse energy. The response $\bar{b}(t)$ is described by the said channel model [7], while the path gain is described by the statistical path loss model [9]. With this we have

$$\alpha = \left(\frac{d}{1\,\mathrm{m}}\right)^{\gamma} 10^{-\frac{PL_0+S}{10}}.$$

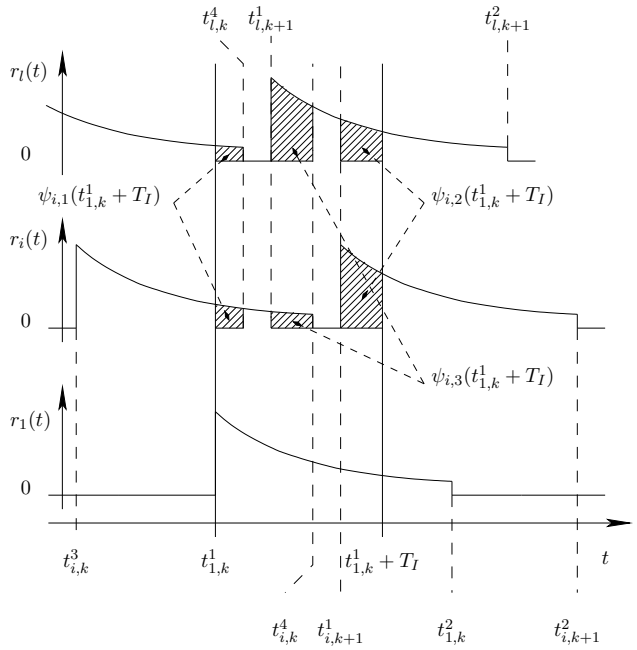

Figure 5: Schematic representation of desired signal $r_1(t)$ and interfering signals $r_i(t)$ and $r_l(t)$ from sensor i and l. In this example there are three separate intervals, indicated by the shaded areas, where the signals $r_i(t)$ and $r_l(t)$ contribute to the mixed interference component, i.e., $\psi_i(t^1_{1,k}+T_I) = \psi_{i,1}(t^1_{1,k}+T_I) + \psi_{i,2}(t^1_{1,k}+T_I) + \psi_{i,3}(t^1_{1,k}+T_I)$.

Where d is the distance between the transmitter and receiver antenna. For a LOS link are given the values distribution of the constants, $PL_0 = 47$ dB, $\gamma = \mathcal{N}(1.7, 0.3)$, and $S = \mathcal{N}(0, \mathcal{N}(1.6, 0.5))$, while for a NLOS link $PL_0 = 51$ dB, $\gamma = \mathcal{N}(3.5, 0.97)$, and $S = \mathcal{N}(0, \mathcal{N}(2.7, 0.98))$.

For a number of N sensors and M cluster heads, there are NM different channel impulse responses denoted as $b_{m,n}(t) = \alpha_{m,n}\bar{b}_{m,n}(t)$, with the sensor index n and the receiver index m; we assume for simplicity and because of lack of better knowledge that the pulse shapes $\bar{b}_{m,n}(t)$ as well as the path gains are statistically independent. We describe the CIR only within the spectrum that is covered by the transmitted signals $\langle u_i(t)\rangle$. The transmitter pulse shape $g(t)$ belongs to an ideal bandpass filter with bandwidth B and center frequency f_0, see Subsection 2.1; thus, we describe the channel only within this passband.

3.1.1 Path Gain and Decay Constant

The realization η, the distribution of the path loss and the exponential decay constant depend on the transmitter to receiver (TR) distance d. The path gain $\alpha_{n,i}$ is chosen according to the model [9]. Because of lack of a more realistic path gain model, we assume that the path gains $\alpha_{n,i}$ for different indices i and j are statistically independent. The path gain and the decay constant are functions of the TR distance d and statistically dependent [10, 9]

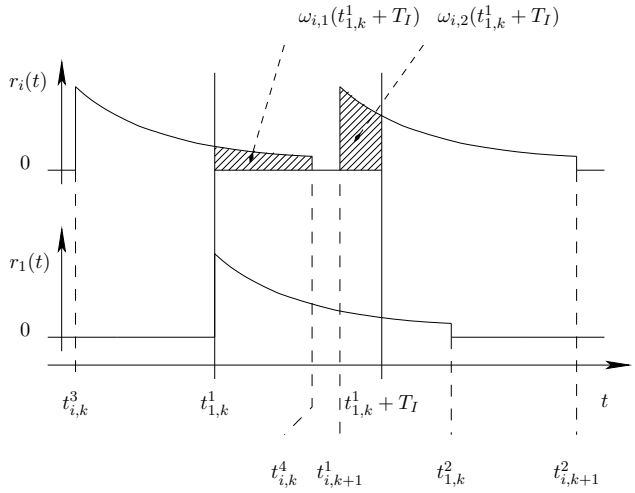

Figure 6: Schematic representation of desired signal $r_1(t)$ and interfering signal from sensor i, $r_i(t)$. In this example there are two time intervals, indicated by the shaded areas, where the signal $r_i(t)$ contributes to the mixed signal-noise component, i.e., $\omega_i(t^1_{1,k}+T_I) = \omega_{i,1}(t^1_{1,k}+T_I) + \omega_{i,2}(t^1_{1,k}+T_I)$.

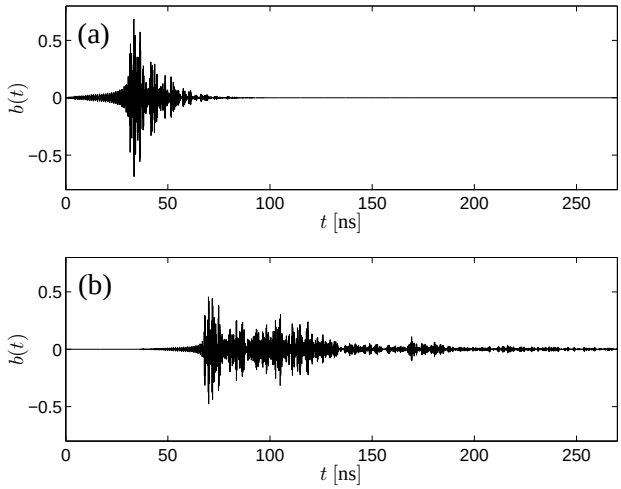

Figure 7: Channel impulse resopnses of (a) CM1 realization one and (b) CM4 realization one. The bandwidth is limited by an ideal bandpass filter with center frequency $f_0 = 4$ GHz and bandwidth $B = 1$ GHz. The energy of these responses is normalized to unity.

3.2 Decision Variable Components

In this section we develop simple approximations for the terms in (4) that rely only on the energy that is captured from the desired signal $r_{j,1}(t)$ and the interfering signals $r_{j,i}(t),\ i \neq 1$. For this analysis, the shape of a received pulse that passed the receiver filter is of particular interest, it is

given by the convolution

$$s_{r,i}(t) = \sqrt{E_t}\, g(t) * b_{m,i}(t) * g(t) = \sqrt{\frac{E_t}{2B}} b_{m,i}(t).$$

3.2.1 Desired Signal Term

$$\begin{aligned}
\nu_n(ts) &= \int_{t_s - T_I}^{t_s} s_{r,1}^2(t)\, dt \\
&= \frac{E_t}{2B} \int_{t_s - T_I}^{t_s} b_{m,n}^2(t)\, dt \\
&= \frac{E_t \alpha_{n,j}}{2B} \int_{t_s - T_I}^{t_s} \bar{b}_{n,j}^2(t) \\
&= \eta_n(T_I) \alpha_{n,j} E_t,
\end{aligned} \tag{6}$$

where $\eta_n(T_I)$ is defined as the ratio or the captured energy per pulse to the received energy per pulse, where the sampling time of the integrator is chosen by the synchronization algorithm such that the captured energy is maximized, i.e.,

$$\begin{aligned}
\eta_n(T_I) &= \max_{t_s} \left\{ \frac{\int_{t_s - T_I}^{t_s} b_{n,i}^2(t)\, dt}{\int b_{n,i}^2(t)\, dt} \right\} \\
&= \max_{t_s} \left\{ \frac{\int_{t_s - T_I}^{t_s} \bar{b}_{n,i}^2(t)\, dt}{\int \bar{b}_{n,i}^2(t)\, dt} \right\} \\
&\max_{t_s} \left\{ \frac{\int_{t_s - T_I}^{t_s} \bar{b}_{n,i}^2(t)\, dt}{2B} \right\}
\end{aligned} \tag{7}$$

3.2.2 Quadratic Interference Term

We express the quadratic interference term $\chi(t_s)$ as a sum

$$\chi(t_s) = \sum_{i=2}^{M} \chi_i(t_s)$$

of terms $\chi_i(t_s) = \int_{t_s - T_I}^{T_I} s_{r,i}^2\, dt$ with the index i indicating the sensor that causes this interference. Zero, one, or two succeeding received pulses of an interfering sensor signal $s_{r,i}$, with $i \neq 1$ can fall into the integration interval $[t_s - T_I, t_s]$. Figure 4 shows an example were two pulses of sensor i fall into this integration interval, i.e.,

$$\chi_i(t_s) = \chi_{i,1}(t_s) + \chi_{i,2}(t_s).$$

The contribution to the quadratic interference term $\chi_i(t_s)$ of any of these pulses depends on the interval where this pulse overlaps with the integration interval. For example if the interfering pulse is nonzero in the interval $[t^1_{i,k}, t^2_{i,k}]$ then, the overlap interval is $t \in [a, b]$ with $a = \max(t^1_{i,k}, t_s - T_I)$ and $b = \min(t^2_{i,k}, t_s)$. The contribution $\chi_{i,1}(t_s)$ of this pulse computes as

$$\begin{aligned}\chi_{i,1}(t_s) &= \int_{t_s-T_I}^{t_s} s^2_{r,i}(t)\,dt \\ &= \frac{E_t\,\alpha_{n,i}}{2B}\int_{t_s-T_I}^{t_s} b^2_{j,i}(\eta, t - t^3_{i,k})\,dt\end{aligned} \tag{8}$$

3.2.3 Mixed Interference Term

Similar as we did to compute the quadratic interference term, we split the mixed interference term into a sum

$$\psi(t_s) = \sum_{i=1}^{M}\sum_{l=1 l\neq i}^{M} \psi_{i,l}(t_s)$$

of terms $\psi_{i,l}(t_s) = \int_{t_s-T_I}^{t_s} s_{r,i}(t)s_{r,l}(t)\,dt$ with the index pair i, l indicating the sensors that cause this interference. With the presented modulation scheme, the integration interval $[t_s - T_I, t_s]$ divides into at most 3 disjoint intervals where a pulse from each, sensor l and a pulse from sensor i collide. i.e. we can write $\psi_{i,l}(t_s) = \psi_{i,l,1}(t_s) + \psi_{i,l,2}(t_s) + \psi_{i,l,3}(t_s)$. Figure 5 shows an example were two pulses of each, sensor i and sensor l fall into this integration interval, such that it splits into three intervals.

The contribution to the mixed interference term $\psi_i(t_s)$ of any of these pulse pairs depends on the interval where they overlap with the integration interval. For example, if the interfering pulses start at the time $t^3_{i,k}$ and $t^3_{l,k}$ respectively, then, the overlap interval is $t \in [a, b]$ with $a = \max(t^3_{i,k}, t^3_{l,k}, t_s - T_I)$, $b = \min(t^4_{i,k}, t^4_{l,k}, t_s)$, and $t_s = t^1_{1,k} + T_I$. The contribution $\psi_{i,l,1}(t_s)$ computes as

$$\begin{aligned}\psi_{i,l,1}(t_s) &= \int_{t_s-T_I}^{t_s} s_{r,i}(t)\,s_{r,l}(t)\,dt \\ &= \frac{E_t}{2B}\sqrt{\alpha_{n,i}\,\alpha_{n,l}}\int_{t_s-T_I}^{t_s} b_{j,i}(\eta, t - t^3_{i,k})\,b_{j,l}(\eta, t - t^3_{l,k})\,dt \\ &= \frac{E_t}{2B}\sqrt{\alpha_{n,i}\,\alpha_{n,l}}\int_{a}^{b} b_{n,i}(t - t^3_{i,k})\,b_{n,l}(\eta, t - t^3_{l,k})\,dt\end{aligned} \tag{9}$$

The other two sums $\psi_{i,l,2}(t_s)$ and $\psi_{i,l,3}(t_s)$ compute similarly but with changed indices as indicated in Fig. 5.

3.2.4 Mixed Signal-Noise Term

The problem of computing the mixed-noise term is from an integration interval perspective equivalent to that of computing the quadratic interference term. Hence, we express the mixed signal-

noise term $\omega(t_s)$ as a sum

$$\omega(t_s) = \sum_{i=2}^{M} \omega_i(t_s)$$

of terms $\omega_i(t_s) = \int_{t_s-T_I}^{T_I} s_{r,i}(t)\, s_n(t)\, dt$ with the index i indicating the sensor that causes this interference.

Furthermore we split the term $\omega(t_s)$ into sums,

$$\omega_i(t_s) = \omega_{i,1}(t_s) + \omega_{i,2}(t_s).$$

According to Fig. 6, see the equivalence with Fig. 4, the term $\omega_{i,1}(t_s)$ computes as

$$\begin{aligned}
\omega_{i,1}(t_s) &= \int_{t_s-T_I}^{t_s} s_n(t)\, s_{r,i}(t)\, dt \\
&= \sqrt{\frac{E_t}{2B}} \int_{t_s-T_I}^{t_s} s_n(t)\, b_{j,i}(t - t_{i,k}^3)\, dt \\
&= \sqrt{\frac{E_t}{2B}} \int_{a}^{b} s_n(t)\, b_{j,i}(t - t_{i,k}^3)\, dt \\
&\sim \mathcal{N}(0, \sigma_\omega^2),
\end{aligned} \tag{10}$$

where $a = \max(t_{i,k}^3,\, t_s - T_I)$ and $b = \min(t_{i,k}^3,\, t_s)$. According to [5] the variance is given by

$$\sigma_\omega^2 = \frac{2\, N_0\, E_t\, \alpha_{n,i}}{2B} \int_a^b \bar{b}_{j,i}^2(t - t_{i,k}^3)\, dt.$$

For $i = n$, i.e. for the desired user signal this is

$$\sigma_\omega^2 = 2\, N_0\, E_t\, \alpha_{n,i}\, \eta_n(T_I).$$

3.2.5 Noise Term

The noise term $\zeta(t_s)$ is gamma distributed as shown in [5], it does not depend on t_s but on the integration duration T_I:

$$f_\zeta(\zeta) = \frac{1}{b^a \Gamma(a)} \zeta^{a-1} e^{-\zeta/b},$$

with $\mu_a = ab$, $\sigma_\zeta^2 = ab^2$ we have

$$a = BT_I$$

and

$$\sigma_\zeta^2 = T_I N_0^2 B.$$

3.3 Detector Input

The decision to detect the symbol sequence of sensor i is based on the decision variable $d_{i,k} = q_{i,k,1} - q_{i,k,2}$. We define

$$t_1 := t_{i,k}^1 + T_I \text{ and } t_2 := t_{i,k}^3 + T_I,$$

with this we have $q_{i,k}^1 = q(t_1)$ and $q_{i,k}^2 = q(t_2)$. When we assume that $a_{1,k} = 0$, evaluating the first integration interval by substituting $t_s = t_1$, we have

$$\begin{aligned} \nu(t_1) &= \eta_n(T_I)\alpha_{n,j}E_t \\ &\sim \text{deterministic} \end{aligned} \tag{11}$$

For the second integration interval with $t_s = t_2$ we have

$$\begin{aligned} \nu(t_2) &= 0 \\ &\sim \text{deterministic} \end{aligned} \tag{12}$$

The following terms do not depend on whether $t_s = t_{i,k}^1 + T_I$ or $t_{i,k}^3 + T_I$:

$$\begin{aligned} \chi(ts) &= \sum_{i=2}^{M} \chi_{i,1}(t_s) + \chi_{i,2}(t_s) \\ &\sim \text{deterministic} \\ \psi(t_s) &= \sum_{i=1}^{M} \sum_{\substack{l=1 \\ l\neq i}}^{M} \psi_{i,l,1}(t_s) + \psi_{i,l,2}(t_s) + \psi_{i,l,3}(t_s) \\ &\sim \text{deterministic} \\ \omega(t_s) &= \sum_{i=1}^{M} \omega_{i,1}(t_s) + \omega_{i,2}(t_s) \\ &\sim \mathcal{N}(0, \sigma_\omega^2(t_s)), \text{ with } \sigma_\omega^2(t_s) = \sum_{i=1}^{M} \sigma_{\omega_{i,1}}^2(t_s) + \sigma_{\omega_{i,2}}^2(t_s), \\ &\quad \text{and } \sigma_{\omega_{i,1}}^2 = \frac{2\,N_0\,E_t\,\alpha_{n,i}}{2B} \int_a^b \bar{b}_{j,i}^2(t)\,dt \\ \zeta(t_s) &\sim \text{Gamma}(\mu_\zeta, \sigma_\zeta^2), \text{ with } \mu_\zeta = T_I\,B\,N_0, \text{ and } \sigma_\zeta^2 = T_I N_0^2 B \end{aligned} \tag{13}$$

With this and for $a_{1,k} = 0$ we find the expression

$$q_{i,k}^1 - q_{i,k}^2 = \nu(t_1) + n_k,$$

with

$$n_k \sim \mathcal{N}\left([\chi(t_1) - \chi(t_2)] + [\psi(t_1) - \psi(t_2)], \sigma_\omega^2(t_1) + \sigma_\omega^2(t_2) + 2\sigma_\zeta^2\right)$$

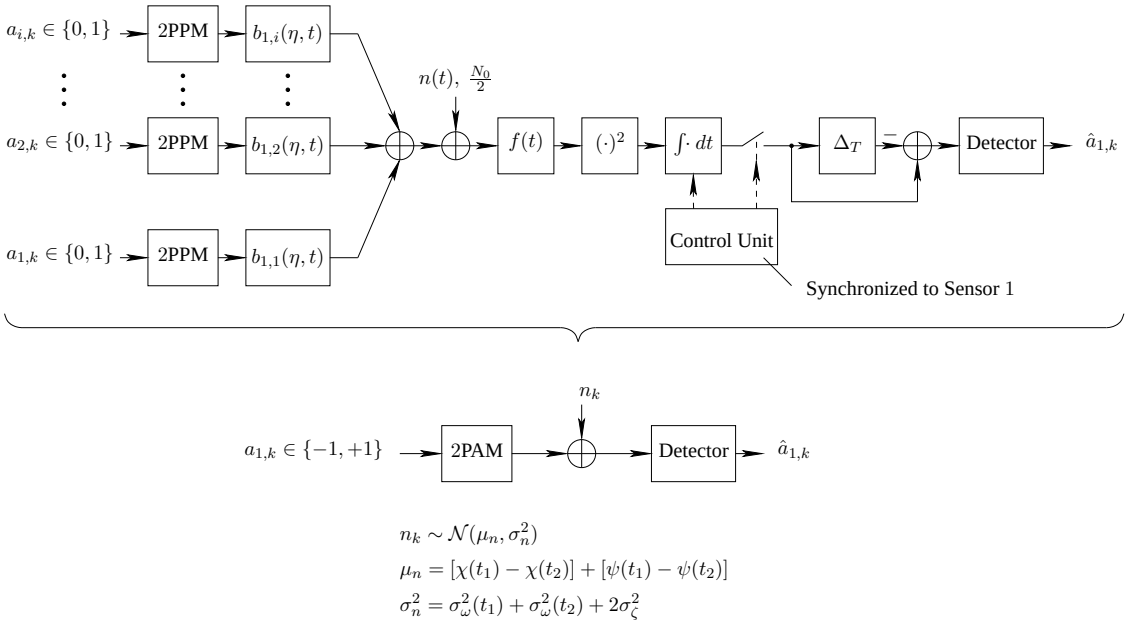

Figure 8: Original and simplified physical layer model.

where we approximated the difference of the two gaussian distributed random variables, $\zeta(t_1)$ and $\zeta(t_2$ by a normal distributed random variable; this approximation holds the better, the larger the product $T_I B$ is [5]. If however $a_{1,k} = 1$ then we find

$$d_k = q_{i,k}^1 - q_{i,k}^2 = -\nu(t_1) + n_k. \tag{14}$$

We observe that this description of the detector input is equivalent to that of a $2PAM$ modulated signal transmitted over a memoryless discrete-time AWGN channel. Hence we have the following description: The symbol alphabet $a_{1,k} \in \{-1, +1\}$ is transmitted over a channel with gain $\nu(t_1)$ and AWGN n_k with nonzero mean and variance , i.e.,

$$d_k = a_{1,k}\nu(t_1) + n_k.$$

The original physical layer model and the derived simplification are illustrated in Fig. 8.

3.4 Effects of Simplification

The most inaccurate aspect of the simplification in this section is the assumption that the difference of two gaussian distributed random variables is gaussian distributed. Small signal bandwidth B, short integration duration T_I and high SNR will result in a simulated BER that is overestimated when compared to the true value.

The assumption of statistically independent path gains will result in an underestimated BER if cluster heads are combined to achieve diversity that combats large scale fading.

Note that the symbol duration T and also the modulation shift Δ_T for 2PPM must both be smaller than the total delay spread of the channel, otherwise intersymbol interference and multiuser interference terms will arise which are not covered by the presented model.

4 Synchronization

A typical radio receiver can synchronize even for SNRs where the bit error rate is about 10^{-2} or 10^{-1}. Therefore a useful but simple method is not to simulate the synchronization procedure, but to assume that the synchronization task was done successively, if the number of symbol errors within a packet's preamble is lower than a fixed threshold.

Acknowledgment

This work was performed within the European IST-FP6 Integrated Project PULSERS (Pervasive Ultra-wideband Low Spectral Energy Radio Systems; Contract No. 506897).

References

[1] W. M. Lovelace and J. K. Townsend, "The effects of timing jitter and tracking on the performance of impulse radio," *IEEE J. Select. Areas Commun.*, vol. 20, no. 9, pp. 1646–1651, Dec. 2002.

[2] R. Hoctor and H. Tomlinson, "Delay-hopped transmitted-reference RF communications," in *Proc. 2002 IEEE Conf. on Ultra Wideband Systems and Technologies*, May 2002, pp. 265–269.

[3] T. Zasowski, F. Althaus, and A. Wittneben, "An energy efficient transmitted-reference scheme for ultra wideband communications," in *IEEE Joint UWBST & IWUWBS 2004*, Kyoto, May 2004, pp. 146–150.

[4] S. Paquelet, L.-M. Aubert, and B. Uguen, "An impulse radio asynchronous transceiver for high data rates," in *IEEE Joint UWBST & IWUWBS 2004*, Kyoto, May 2004, pp. 1–4.

[5] M. Weisenhorn and W. Hirt, "Robust noncoherent receiver exploiting UWB channel properties," in *IEEE Joint UWBST & IWUWBS 2004*, Kyoto, May 2004, pp. 156–160.

[6] R. Merz, J. Widmer, J. Y. Le Boudec, and B. Radunovic, "A joint phy/mac architecture for low-radiated power th-uwb wireless ad-hoc networks," *Wireless Communications and Mobile Computing Journal, Special Issue on Ultrawideband (UWB) Communications*, June 2005.

[7] J. Foerster. (2003, Feb.) Channel Modeling Sub-committee Report Final. 02490r1P802-15. [Online]. Available: http://grouper.ieee.org/groups/802/15/pub/2003/Mar03/

[8] M. Weisenhorn and W. Hirt, "Impact of the FCC average- and peak power constraints on the power of UWB radio signals," Research Report RZ3544, IBM Zurich Res. Lab., Sept. 2004.

[9] S. S. Ghassemzadeh, R. Jana, C. W. Rice, W. Turin, and V. Tarok, "A statistical path loss model for in-home UWB channels," in *Proc. 2002 IEEE Conf. on Ultra Wideband Systems and Technologies*, May 2002.

[10] K. Siwiak, H. L. Bertoni, and S. M. Yano, “Relation between multipath and wave propagation attenuation,” *IEE Electronic Letters*, vol. 39, no. 1, pp. 142–143, Jan. 2003.